Carbon – Science and Technology

ARTICLE

Magnetic properties of electroless nickel-phosphorus coated multi-walled carbon nanotubes

Amanda V. Ellis [*, A]**, James Storey** [B]**, Samuel Wallace** [A]**, Bridget Ingham** [B]

(A) School of Chemistry, Physics and Earth Sciences, Flinders University, Sturt Road, Bedford Park, Adelaide, S.A 5042, Australia.
(B) Nanotechnology Platform, Industrial research Ltd, Gracefield Road, Lower Hutt, Wellington, New Zealand.

Nickel-phosphorus (EN) deposited multi-walled carbon nanotubes (MWCNTs) were prepared using an electroless plating technique. The D.C and A.C magnetic behavior of the composites showed that pre-acid treatment of the MWCNTs prior to electroless deposition greatly enhanced the magnetic susceptibility at 5 K producing a composite with antiferromagnetic correlations and a superparamagnetic transition at 65.5 K. Raman scattering analysis suggests that there is no direct interaction of the nickel-phosphorus deposit and the MWCNTs.

----

1. Introduction :

Electrochemically deposited nickel-phosphorus via an electroless process exhibits many unusual physical properties which include good hardness, wear resistance, ferromagnetic to paramagnetic transitions [1-3], and high conductivity [4]. Its deposition onto a variety of substrates such as, SiO_2 [5,6], carbon [7,8] and carbon nanotubes (CNTs) [9,10] is of particular interest in areas of catalysis [11], wear resistant coatings [9], anti-corrosive coatings [12] and magnetic data storage [1,3].

Attention is being paid to carbon nanotubes as a substrate not only as they afford a large surface area but also as they provide additional unique physical properties to the composite, such as mechanical strength, thermal conductivity and magnetic properties. Applications include nanowire interconnects, transistors, ultra-capacitors and high-tensile nanotechnology in the electronics industries. In order to make CNTs useful as individual nanowires the van der Waals interactions between neighboring tubes in bundles of pristine material need to be broken. This is most usually achieved through surface oxidation of side wall and edge-plane sp^3 moieties and typically involves the sonication or reflux of the CNTs in concentrated acids, such as H_2SO_4 and HNO_3 [13-15]. Through this method of oxidation the van der Waals interactions are removed and the CNTs become more dispersed and water-soluble [13-15]. Oxidation can also occur at topological defects, such as Stone-Wales defects (SWDs), pairs of pentagon-heptagon localized states [16]. The formation of these oxidised moieties is highly dependent on the orientation, chirality and radius of the tube [17] and these sites may offer some advantage to the sequestering and subsequent nucleation of Ni-P deposits. Deposition onto carbon nanotubes is a

relatively new field and the effect the nanotube surface plays on the Ni-P deposition is not yet understood.

Electroless Ni-P plating onto CNTs has been previously shown by Shen et al. [9,10] who successfully plated a pristine CNT placed on an electrochemical microactuator. Ramaseshan et al. [18] have shown an increase in magnetization of Ni-P when plated onto Ti and Al powders. Chen et al. [19] have reported on the magnetic coecivity of electroless deposits of Co nanoparticles on CNTs, finding an enhancement compared to bulk Co. To our knowledge their have been no reports on the magnetic properties of electroless nickel plated acid treated multi-walled carbon nanotubes.

This work reports on the difference in the magnetic properties of an electroless Ni-P deposit on pristine and acid treated carbon nanotubes. Initially it was proposed that the introduction of functional groups such as carbonyl, carboxylic groups, and phenolic groups onto the surface of the otherwise inert CNTs would introduce nucleation sites for metal deposition. This does not appear to be the case in the work shown here. While HRTEM and XPS show deposition of Ni-P onto the surface of the CNTs the Raman spectroscopy results indicate that there is no chemical or electronic interaction between the Ni-P deposit and the oxidised defect states. Magnetic measurements using a SQUID magnetometer clearly show that Ni-P deposited onto, in particular, acid treated CNTs results in enhancement of the mass susceptibility (at 5 K) and antiferromagnetic correlations with a superparamagnetic transition at 65.5 K.

2. Experimental :

Multi-walled carbon nanotubes (MWCNTs) (<10 nm, 5-15 μm in length, and ≥95% purity) were purchased from

Shenzhen Nanotech Port Co., Ltd. (Nanoport - NTP), China and produced by the catalytic decomposition of CH_4 using La_2NiO_4 as a catalyst precursor. An acid oxidative method [13,15] was used to render the MWCNTs more water soluble and remove any residual catalyst particles. This involved acid treating the MWCNTs (500 mg) by reflux in a round bottom flask with concentrated sulphuric acid (15 mL) and concentrated nitric acid (5 mL) for 68 h at 120 °C. The mixture was then cooled and diluted with MilliQ water (500 mL). The resulting suspension was then filtered under vacuum through a 0.45-μm PTFE Whatman micro-filter paper and thoroughly washed with MilliQ water until the outlet was neutral to pH paper.

Electroless nickel-phosphorus (EN) deposition of the pristine MWCNTs and acid-treated-MWCNTs was achieved by using a commercial autocatalytic hypophosphite bath (ENPLATE NI-425 by ENTHONE-OMI (Australia)). This solution was used as supplied. MWCNTs (10 mg) were placed in 10 mL of ENPLATE NI-425 solution (pH 4.80) and the solution was heated with stirring at 86 °C for 2 h. The MWCNTs were then filtered out under vacuum through 0.45-μm PTFE Whatman micro-filter paper and thoroughly washed with MilliQ water.

Ni-P plated pristine MWCNTs and Ni-P plated acid-treated-MWCNTs were dispersed in a toluene medium and transferred to a carbon-coated Cu-grid for high-resolution transmission electron microscopy (HRTEM) measurements in a JEOL-2010 TEM operated at 200 kV. Energy dispersive X-ray spectroscopy (EDS) was also performed on the non-plated pristine and Ni-P plated acid-treated-MWCNTs using STEM with high spatial resolution (~2-10 nm). For X-ray photoelectron spectroscopy (XPS) analysis a control sample of Ni-P deposited onto a glass slide with a thermally evaporated gold surface was fabricated. A sample also measured was the Ni-P plated acid-treated-MWCNTs. A Perkin-Elmer (PHI) surface analysis chamber (1x 10^{-10} torr) with cylindrical mirror analyser equipped with a monochromatized Al Kα X-ray source (1486.6 eV, 240W, 14 kV) was used to obtain spectra. A constant pass energy of 50 eV was used for all scans with a step-size of 0.1 eV was used. All spectra were referenced to the C 1s peak at 284.6 eV for highly orientated pyrolytic graphite (HOPG).

A Quantum Design MPMS XL SQUID magnetometer was used to measure the DC magnetization of the different samples. A sample of 5-10 mg was sealed in a small gelatin capsule with a negligible magnetic contribution. Hysteresis loops between ±7 Tesla performed at 5 K and 77 K after cooling the sample in zero applied field. The magnetization of the four samples was measured for fields from 0 to 6 Tesla at temperatures of 5 K and 77 K.

The mass susceptibility of the Ni-P plated acid-treated-MWCNTs was measured using field-cooled and zero-field-cooled temperature sweeps from 5 K to 305 K at 0.0015 Tesla. The AC susceptibility of the Ni-P plated acid-treated-MWCNTs was measured at temperatures from 5 K to 305 K. The measurements were taken under applied fields with 2 Oe amplitude and frequencies of 33, 180, 430 and 822 Hz.

Raman scattering analysis was carried out by placing dried samples onto a silicon wafer and using microscope laser Raman spectroscopy with a Jobin Yvon-LabRam HR spectrometer. The laser excitation was 632.8 nm (1.96 eV) with a spectral resolution of 1.5 cm^{-1}.

3. Results and discussion :

3.1 High resolution transmission electron microscopy (HRTEM) analysis :

Figure (1) shows a representative HRTEM image of EN deposited acid-treated-MWCNTs. The inset shows the absence of any basal planes typically observed from the outer walls of MWCNTs due to an amorphous coating covering the entire nanotube. An amorphous deposit is expected if the phosphorus content of the nickel phosphide is greater than 10 % [20]. EDS analysis was used to determine the chemical composition of the coating on the MWCNTs showing the presence of phosphorus (1.02 wt%, 0.40 at%) and nickel (1.23 wt%, 0.26 at%). This indicates that the nickel deposit is phosphorus rich and thus the Ni-P compound should be amorphous [20].
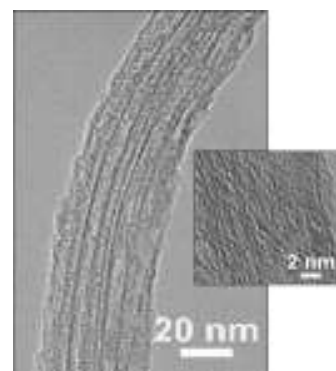

Figure (1) : HRTEM images of Ni-P plated pristine-MWCNTs. Inset: expanded region of Ni-P plated pristine-MWCNTs basal planes.

3.2 X-ray photoelectron spectroscopy (XPS) analysis :

A reference sample was produced by the electroless deposition of Ni-P onto a freshly cleaned glass slide which had been pre-coated with thermally evaporated gold. An XPS survey scan of the Ni-P deposit is shown in Figure (2).
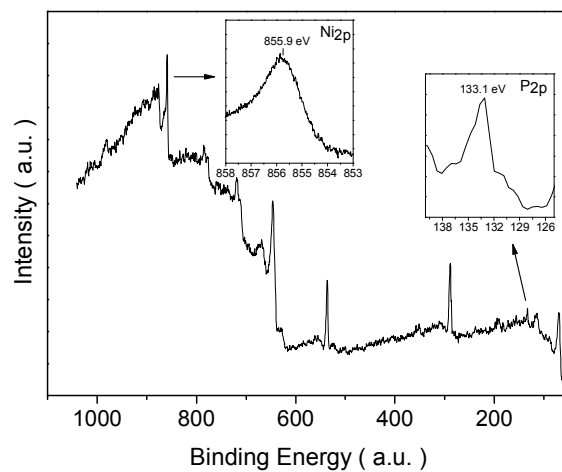

Figure (2) : XPS survey spectrum of a Ni-P deposit on a gold slide. Inset shows Ni$_{2p}$ and P$_{2p}$ peaks.

The insets show the intense $2P_{3/2}$ Ni peak (B.E = 855.9 eV) and the lower intensity $2P_{3/2}$ P^0 peak (B.E = 133.1 eV) and $2P_{1/2}$ P^0 shoulder associated with the Ni-P alloy.

Figure (3) shows the Ni_{2p} region spectra after Ni-P is plated onto acid treated MWCNTs. A doublet appears at B.E 859.1 eV and 863.6 eV with a 4.5 eV separation in energy. This indicates that the Ni^0 exists as a mixture of nickel oxide, hydroxide, phosphide or phosphates [231. The phosphorus peak was unable to be resolved.
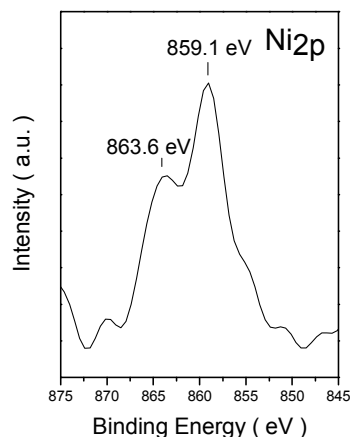

Figure (3) : XPS survey spectrum of the Ni_{2p} peak of Ni-P plated acid-treated-MWCNTs.

3.3 D.C and A.C magnetization :

In order to study the differences in magnetic properties of Ni-P plated pristine-MWCNTs and Ni-P plated acid treated MWCNTs magnetic susceptibility readings were taken. A comparison firstly of Ni-P plated and non-plated pristine material was carried out. Magnetic hysteresis plots for pristine-MWCNTs at 77 K (solid squares) and 5 K (open squares) and Ni-P deposited pristine-MWCNTs at 77 K (solid circles) and 5 K (open circles) are shown in Figure (4). Magnetization is plotted per mass of MWCNT versus applied field. The saturation magnetization at 77 K for the Ni-P plated and non-plated pristine-MWCNTs is approximately the same, occurring at 2.2 emu/g.
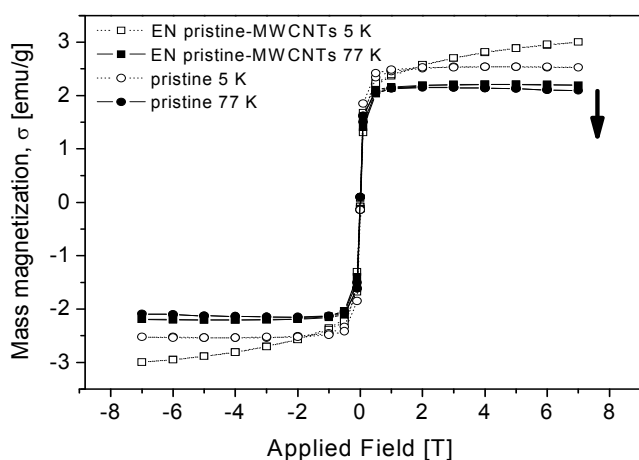

Figure (4) : Hysteresis loops for pristine MWCNTs (●-) and Ni-P plated pristine-MWCNTs (■-) obtained at 77 K (solid line solid symbol) and 5 K (dotted line open symbol).

The only difference here is that the pristine material has a slight diamagnetic response (indicated by arrow in Figure 4), typical of carboneous materials and their paired electrons [22]. At 5 K there is a significant difference in the saturation magnetization between the plated and non-plated pristine-MWCNTs. For the non-plated pristine-MWCNTs the saturation magnetization is 2.5 emu/g, at approximately 1 Tesla. In contrast to the plated pristine-MWCNTs which never reach a saturation magnetization even at 7 T (3 emu/g). For bulk nickel at room temperature the magnetization is 54.4 emu/g [23]. The notable reduction in magnetization compared to bulk nickel is often observed in nanoparticles due to the large percentage of surface spins that have disordered magnetization orientation [24]. Neither samples shows any coercive field or remnant magnetization. CNTs that had been acid treated prior to Ni-P plating showed the most unusual behavior. Figure (5) shows the non-plated acid-treated-MWCNTs at 77 K (closed circles) and 5 K (open circles) – these appear overlaid in the plot - and the Ni-P plated acid-treated-MWCNTs at 77 K (closed squares) and 5 K (open squares). Comparison of the saturation magnetization at 77 K of the non-plated pristine (Figure 4) and non-plated acid treated (Figure 5) clearly shows a reduction after acid treatment, 2.2 emu/g to 0.33 emu/g, respectively. This reduced magnetization is an indication that catalytic compared to bulk nickel is often observed in nanoparticles due to the large percentage of surface spins that have disordered magnetization orientation [24].
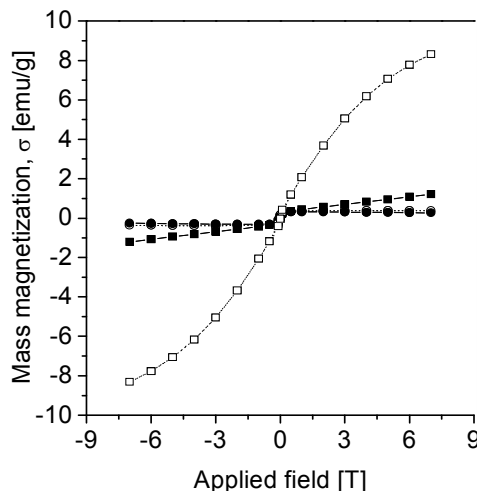

Figure (5) : Hysteresis loops for 68 h acid treated (●-) and EN deposit on acid-treated-MWCNTs (■-) obtained at 77 K (solid line solid symbol) and 5 K (dotted line open symbol).

After Ni-P plating the acid treated nanotubes the mass magnetization does not saturate at 7 K and increases linearly (Figure 5 closed squares) to 1.4 emu/g at 7 T. This response is not dissimilar for the Ni-P plated pristine material, 2.2 emu/g at 7 K. However at 5 K the response is very different (Figure 5 open squares) in which the mass magnetization increases non-linearly to 8.3 emu/g at 7 T compared to 3.3 emu/g for the Ni-P plated pristine-MWCNTs. To investigate this effect further temperature-dependent mass susceptibility measurements where carried out on the Ni-P plated acid-treated MWCNTs. Figure (6a) shows the mass susceptibility versus temperature data obtained. The field-cooled (FC)

plot shows the mass susceptibility increases monotonically with decreasing temperature. Upon zero-field cooling the sample shows superparamagnetic behavior with the appearance of a peak at lower temperatures. This is the blocking temperature (T_B), seen here at 65.5 K. The blocking temperature depends on the shape and size of the Ni-P deposit and usually increases with the number of atoms. Below this blocking temperature divergence occurs because the spins from each Ni-P are in alignment with the easy crystalline axis that is closest to the applied field direction, and remain frozen in that direction at low temperatures. Below T_B the FC magnetization increases, indicative of superparamagnetic behavior. Above T_B in the absence of any external magnetic field (ZFC), the magnetization direction of the Ni-P atoms fluctuates randomly.

Figure (6b) shows the reciprocal of the mass susceptibility versus temperature plot for the field cooled data. Linear fitting shows the Ni-P plated acid-treated-MWCNTs have a Curie Weiss temperature of -101.6 ℃, indicating the presence of antiferromagnetic (AF) correlations. In contrast the Curie Weiss temperature for pure bulk nickel which is ferromagnetic is 627 K [25]. Antiferromagnetic nanoparticles have had their permanent magnetic moment attributed by Néel to an uncompensated number of spins in the two sublattices [26]. In low-dimensional materials of only a few monolayers in thickness, the surface anisotropy often dominates, resulting in magnetization perpendicular to the surface [27]. Therefore the superparamagnetism observed here may be attributed to surface anisotropy. That is, the spins at the surface of the Ni-P deposit are unbalanced and while the Ni-P core is tending towards AF correlations, the surface spins are aligning with the field. At sufficiently low temperatures and/or high fields, the signal from the surface effect becomes greater than the bulk.

The resulting superparamagnetism arises due to the lack of 3-dimensonsal magnetic order, as a result of this surface effect. It is apparent that acid treatment has contributed to the increase in the Ni-P deposits surface anisotropy.
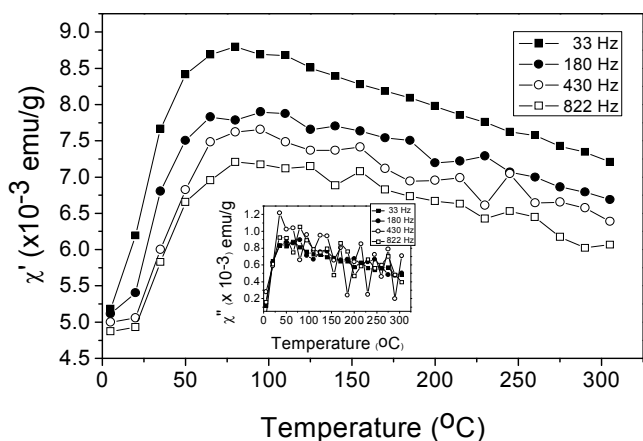

Figure (6) : (a) Temperature dependence of mass susceptibility for an applied field of 0.0015 T obtained for Ni-P plated acid-treated-MWCNTs after zero-field cooling (circles) and field cooling (squares); (b) shows the reciprocal of the mass susceptibility versus temperature plot for the field cooled data.

Figure (7) shows the real (χ') part of the A.C susceptibility of the Ni-P plated acid-treated-MWCNTs. The magnitude of χ' decreases as the frequency increases and as the frequency is increased χ' is suppressed below the T_B (65 K). This is characteristic behavior of superparamagnets and spin glasses [28]. In this case it is unlikely to be a spin glass because there is no frequency-dependence in the χ'' peak position and more likely its origin is attributed to dipole interactions among particle moments (or superspins) [28]. The peak temperatures are independent of frequency maximizing at approximately 75 K. Figure (7) inset shows the imaginary (χ'') part of the A.C susceptibility.

From this it is observed that below the peak temperature it is frequency independent. Jonsson et al. [29] assign this to interparticle interaction, which inhibits spin relaxation at low temperatures.
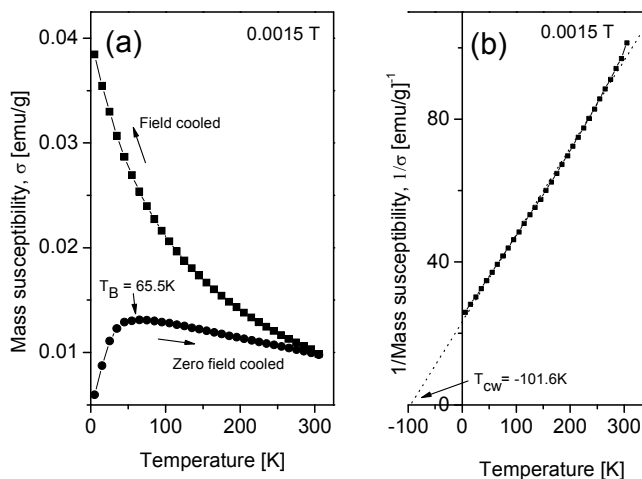

Figure (7) : Temperature and frequency dependence of the real part (χ') of A.C susceptibility of Ni-P plated acid treated-MWCNTs. Inset: shows the imaginary (χ'') part of the A.C susceptibility.

3.4 Raman scattering analysis :

Figure (8a-8c) shows the Raman scattering spectra of pristine, acid treated and Ni-P plated acid-treated-MWCNTs, respectively. The spectra show two main peaks from the D-band, associated with the disordered or amorphous carbon ($\upsilon \approx 1350$ cm^{-1}) and the G-band, associated with the graphitic carbon in MWCNTs ($\upsilon \approx 1582$ cm^{-1}). Figure (8a) shows the G-band of the pristine material as centered at 1582 cm^{-1} after acid treatment (Figure 8b). The G-band is reduced in intensity and shifted to 1594 cm^{-1}. The G-band regularly shifts to blue upon p-doping (anodic charging) which reflects the stiffening of the graphene mode if holes are introduced into the π band [30]. The blue-shift per hole ($\Delta\omega/\Delta f$) was reported to be 320 cm^{-1} [30]. After acid treatment a shoulder appears on the G-band at $\upsilon = 1621$ cm^{-1} and can be assigned to the disorder-induced disorder mode (D'-band), a result of the formation of oxidized sp^3 moieties on the nanotube surface [15,17]. The spectrum of the Ni-P plated acid-treated-MWCNTs (Figure 8c) shows very little change from the acid treated MWCNT spectrum.
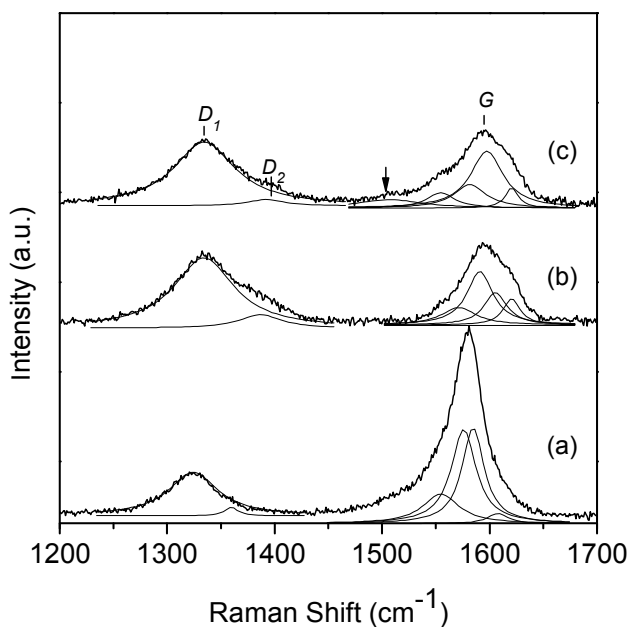
Figure (8) : Raman scattering spectra at E_{laser} = 632 nm for (a) pristine MWCNTs, (b) acid treated MWCNTs, and (c) Ni-P plated acid-treated-MWCNTs.

The fact that the disorder-induced disorder peak at υ = 1621 cm^{-1} is unchanged it significant and implies that there is no chemical bonding or electronic interaction between the oxygen moieties and the Ni-P. Clearly, there must be another reason for the enhancement in magnetisation between untreated and treated nanotube surfaces which needs to be further investigated.

4. Conclusions :

We report a simple economic process for electroless nickel-phosphorus (EN) deposition onto high surface area multi-walled carbon nanotubes (MWCNTs). The EN deposit is shown to be amorphous and high in phosphorus. Raman scattering showed that the acid treated-EN MWCNTs did not change the disorder-induced disorder band (D' at 1621 cm^{-1}). This indicates that EN deposition is not at these localized sites but may be through intercalation or impregnation between intershells. After Ni-P plating the acid treated nanotubes the mass magnetization does not saturate at 7 K and increases linearly (Figure 5 closed squares) to 1.4 emu/g at 7 T. This response is not dissimilar for the Ni-P plated pristine material. However at 5 K the response is very different (Figure 5 open squares) in which the mass magnetization increases non-linearly to 8.3 emu/g at 7 T compared to 3.3 emu/g for the Ni-P plated pristine-MWCNTs. A study of the D.C and A.C magnetic behavior of this material using SQUID found that in the case of the acid treated MWCNTs after EN deposition the Ni-P deposited alloy showed antiferromagnetic correlations with a superparamagnetic transition at 65.5 K.

References :

[1] I. Bakonyi, A. Burgstaller, W. Socher, J. Voitländer, E. Tóth-Kádár, A. Lovas, H. Ebert, E. Wachtel, N. Willmann,, H.H. Liebermann, Phys. Rev. B 47 (1993) 14961.

[2] M.–K. Chang, C.–H. Chen, B.–H. Chen, J. Magn. Magn. Mater. 305 (2006) 342.

[3] J. Park, B. Koo, K.Y. Yoon, Y. Hwang, M. Kang, J.–G. Park, T. Hyeon J. Am. Chem. Soc. 127 (2005) 8433.

[4] J.P. Carini, S.R. Nagel, Phys. Rev. B 27 (1982) 7589.

[5] S. Yang, R. Prins, Chem. Commun. (2005) 4178.

[6] S.J. Sawhill, D.C. Phillips, M.E. Bussell, J. Catal. 215 (2003) 208.

[7] Y. Shu, S.T. Oyama, Carbon 43 (2005) 1517.

[8] Y. Shu, S.T. Oyama, Chem. Commun. (2005) 1143.

[9] G.–R. Shen, L.–N. Tsai, T.–Y. Chao, Y.T. Cheng, T.K. Lin, W. Hsu, 4th IEEE Conference on Nanotechnology (2004) 192.

[10] G.–R. Shen, Y.–T. Cheng, L.–N. Tsai, IEEE Transactions on Nanotechnology 4 (2005) 539.

[11] S.T. Oyama, Y.K. Lee, J. Phys. Chem. B 109 (2005) 2109.

[12] R.L. Zeller III, L. Salvati Jr, Corrosion 50 (1994) 457.

[13] S.A. Curran, A.V. Ellis, K. Vijayaraghavan, P.M. Ajayan, J. Chem. Phys. 120 (2004) 4886.

[14] A.V. Ellis, K. Vijayamohanan, R. Goswami, N. Chakrapani, L.S. Ramanathan, P.M. Ajayan, G. Ramanath, Nano. Lett. 3 (2003) 279.

[15] A.V. Ellis, A. Bubendorfer, Chem. Phys. Lett. 412 (2005) 449.

[16] J.C. Charlier, Acc. Chem. Res. 35 (2002) 1063.

[17] C. Pan, W.S. Yang, J. Yang, Phys. Rev. B 62 (2000) 12652.

[18] R. Ramaseshan, S.K. Seshadri, N.G. Nair, Scripta Mater. 45 (2001) 183.

[19] X. Chen, J. Xia, J. Peng, W. Li, S. Xie, Compos. Sci. Techol. 60 (2000) 301.

[20] M. Lidun, L. Kang, S. Xiaoliang, Physica B 158 (1989) 692.

[21] B.C. Zhang, G. Barth, H.K. Liu, S. Chang, Appl. Surface Sci. 231-232 (2004) 868.

[22] A.V. Ellis, B. Ingham, J. Magn. Magn. Mater. 302 (2006) 378.

[23] C. Kittel, Introduction to Solid State Physics, seventh ed. (New York:Wiley) 1996.

[24] H.R. Kodoma, A.E. Berkovitz, E.J. McNiff Jr, S. Foner, Phys. Rev. Lett. 77 (1996) 394.

[25] S. Chikazumi, Physics of magnetism (New York:Wiley) 1964.

[26] L. Néel In: Low Temp. Phys. Eds. C. Dewitt, B. Dreyfus, P.D. de Gennes, (New York: Gordon and Beach) 1962, p. 413.

[27] M. Farle, B. Mirwald-Schulz, A.N. Anisimov, W. Platow, K. Baberschke, Phys. Rev. B 55 (1997) 3708.

[28] M. Sasaki, P.E. Jönsson, H. Takayama, H. Mamiya, Phys. Rev. B 71 (2005) 04405.

[29] T. Jonsson, P. Nordblad, P. Svedlindh, Phys. Rev. B 57 (1998) 497.

[30] L. Kavan, P. Rapta, L. Dunsch, M.J. Bronikowski, P. Willis, R.E. Smalley, J. Phys. Chem. B 105 (2001) 10764.